# Magnetic-statetuning of the rhombohedralgraphitefilm by interlayerspacing and thickness

| | |
|---|---|
| 著者別名 | 岡田 晋 |
| journal or publication title | Surface science |
| volume | 606 |
| number | 3-4 |
| page range | 253-257 |
| year | 2012-02 |
| 権利 | (C) 2011 Elsevier B.V.<br>NOTICE: this is the author's version of a work that was accepted for publication in Surface Science. Changes resulting from the publishing process, such as peer review, editing, corrections, structural formatting, and other quality control mechanisms may not be reflected in this document. Changes may have been made to this work since it was submitted for publication. A definitive version was subsequently published in PUBLICATION, Volume 606(3 4),2012, DOI:10.1016/j.susc.2011.10.001 |
| URL | http://hdl.handle.net/2241/116760 |

doi: 10.1016/j.susc.2011.10.001

# Magnetic-state tuning of the rhombohedral graphite film by interlayer spacing and thickness

Nguyen Thanh Cuong[a,c,*], Minoru Otani[a,c], Susumu Okada[b,c]

[a] *Nanosystem Research Institute, National Institute of Advanced Industrial Science and Technology (AIST), Tsukuba 305-8568, Japan*
[b] *Graduate school of Pure and Applied Sciences, University of Tsukuba, 1-1-1 Tennodai, Tsukuba 305-8571, Japan*
[c] *Japan Science and Technology Agency, CREST, 5 Sanbancho, Chiyoda-ku, Tokyo 102-0075, Japan*

**Abstract**

Based on first-principles total-energy calculations, we systematically investigate how the electronic and magnetic properties of rhombohedral graphite thin films depend on the interlayer spacing and number of layers. Our calculations show that the magnetic ordering of the thin films depends on the interlayer spacing. Thin films under compression normal to the layers possess finite magnetic moments, indicating parallel spin coupling between the two surfaces. We also find that thin graphite films with seven or more atomic layers exhibit magnetic ordering while films with six or less atomic layers are metallic with no magnetic ordering.

*Keywords:* Rhombohedral graphite, Magnetism, Interlayer spacing, Thickness

## 1. Introduction

Boundary conditions imposed on graphene are known to induce interesting variation in the geometric and electronic properties of the resultant materials: a periodic boundary condition leads to the nanometer scale tubular form of carbon, with electronic properties ranging from semiconducting to metallic depending on the atomic arrangement around the circumference

*Corresponding author
*Email address:* cuong-nguyen@aist.go.jp (Nguyen Thanh Cuong)

[1, 2]; in contrast, an open boundary condition leads to one-dimensional graphene nanoribbons, whose electronic structures sensitively depend on the edge atomic arrangement and width [3, 4]. Early theoretical work pointed out that ribbon with zigzag edges possesses a peculiar edge localized state, forming half-filled flat dispersion bands in part of the one-dimensional Brillouin zone [5, 6, 7]. It has also been pointed out that these flat bands cause ferromagnetic spin ordering along the edge along with antiferromagnetic coupling between edges.

Besides the boundary condition on the covalent network of C atoms of graphene, the mutural arrangement on the stacking direction can also induce peculiar electronic states at the Fermi level and affect the magnetic ordering of the surfaces of graphite [8, 9, 10, 11]. By imposing an open boundary condition normal to the stacking direction of graphite with a rhombohedral stacking arrangement, the flat dispersion bands emerge at the vicinity of the $K$ point, and have a surface localized nature as in the case of the edge state of graphene ribbon with zigzag edges. As a result of the flat band, the (0001) surfaces of rhombohedral graphite exhibit ferrimagnetic spin ordering with a magnetic moment of 0.036 $\mu_{\rm B}/{\rm nm}^2$ [10]. Further analysis has revealed that the polarized electron spins are coupled in antiparallel between the topmost and the bottommost surfaces of the slab. A previous analysis corroborates the fact that the edge state is the common characteristic on the surface or edges of various materials with particular symmetries [12].

Recent theoretical work has pointed out that the extent of the flat band region of the edge state strongly depends on the unisotropic electron transfer among the atomic sites. For instance, on the (111) surfaces of diamond lattice, the flat band region extends across one fourth of the $K$-$\Gamma$ line [13]. However, on the (0001) surfaces of rhombohedral graphite thin film, which can be regarded as highly anisotropic versions of the (111) surfaces of diamond, our previous calculation indicated that the flat band states emerge only in the vicinity of the $K$ point. Furthermore, the flat band region strongly depends on the electron transfer along the interlayer direction of graphite thin film [10]. Thus, the purpose of this work is to unravel the electronic structure and magnetic states of thin films of rhombohedral graphite with (0001) surfaces in terms of the interlayer spacing and the thickness. Our calculations based on the first-principles total-energy calculations in the framework of the density functional theory (DFT) indicate that the magnetic properties of thin films of rhombohedral graphite strongly depend on their interlayer spacing, which directly affects the interlayer electron transfer. Furthermore, we also

show that the slab thickness affects the electronic properties of graphite thin films.

## 2. Computational Details

All calculations have been performed based on the density functional theory [14, 15]. We used the local spin density approximation (LSDA) to treat the exchange-correlation potential of interacting electrons [16, 17]. Ultrasoft-pseudopotential was adopted to describe the electron-ion interaction [18]. The valence wave functions and charge density were expanded in terms of a plane-wave basis set with cutoff energies of 25 Ry and 324 Ry, respectively. We considered thin films of graphite with rhombohedral (ABCA) stacking comprising three to thirteen graphene layers. For each thin film, the interlayer spacing between graphene layers is varied from 2.7 to 3.4 Å. In the repeated slab model, each thin film is separated from its periodic image by a 12 Å vacuum region. In the lateral directions, we used 1×1 periodicity with two C atoms in each graphene layer. To avoid periodic image errors arising from the repeated slab model, we adopted the effective-screening medium method [19, 20]. Because of the narrowness of the flat-band region in the Brillouin zone which affects the magnetic properties, we used fine k-point sampling of 52×52 equidistant $k$-points mesh for the surface Brillouin zone integration.

## 3. Results and discussion

We first investigated the dependency of the magnetic ordering of the graphite thin films on their interlayer spacing. Figure 1 shows the contour plots of the electron spin density ($\Delta\rho = \rho_\uparrow - \rho_\downarrow$) of rhombohedral graphite thin films with eight atomic layers at various interlayer spacings. As shown in Fig. 1(a), the spin density on the topmost or bottommost surfaces exhibits ferrimagnetic ordering. At the same time, between the two surfaces, the spins are coupled in an antiparallel way as was found for the spin density of graphene ribbon with zigzag edges. Because of this antiparallel spin configuration between the surfaces, the net spin moment of the thin films is zero. For films with moderate interlayer spacing, the magnetic ordering maintains the characteristics observed at equilibrium interlayer spacing [Figs. 1(b)-1(c)]. However, upon further decrease in the interlayer spacing, the spin density

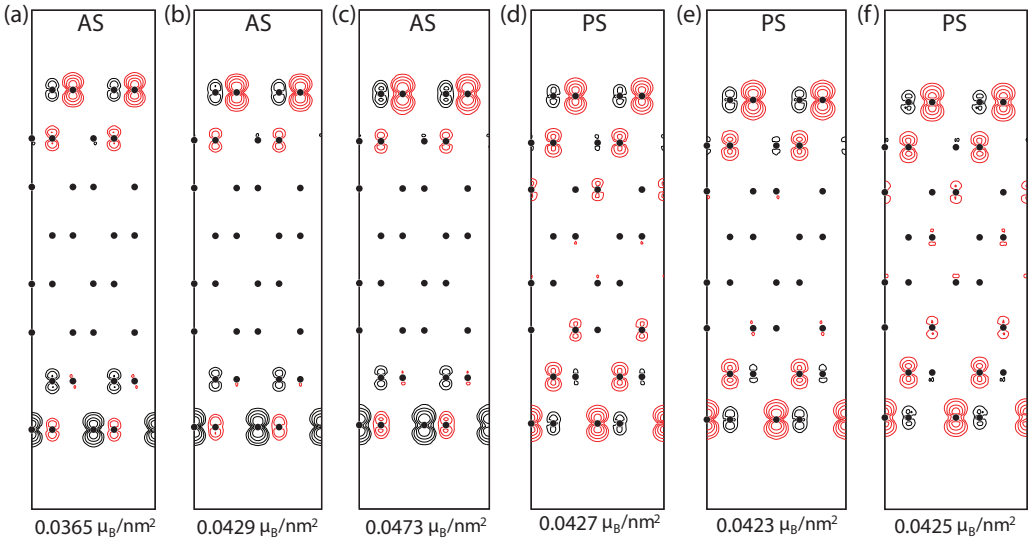


Figure 1: Contour plots of spin density, and surface magnetic moment ($\mu_{\rm B}/{\rm nm}^2$) of eight atomic layer rhombohedral graphite slabs at various interlayer spacings: (a) d=3.35 Å, (b) d=3.2 Å, (c) d=3.10 Å, (d) d=3.00 Å, (e) d=2.80 Å, and (f) d=2.70 Å. The solid circles denote the position of C atoms. Positive and negative values of spin density are shown by red (gray) and black lines, respectively. Each contour represents twice (or half) the density of adjacent contour lines. AS and PS symbols denote antiparallel and parallel coupling spin states of topmost and bottommost layers, respectively.

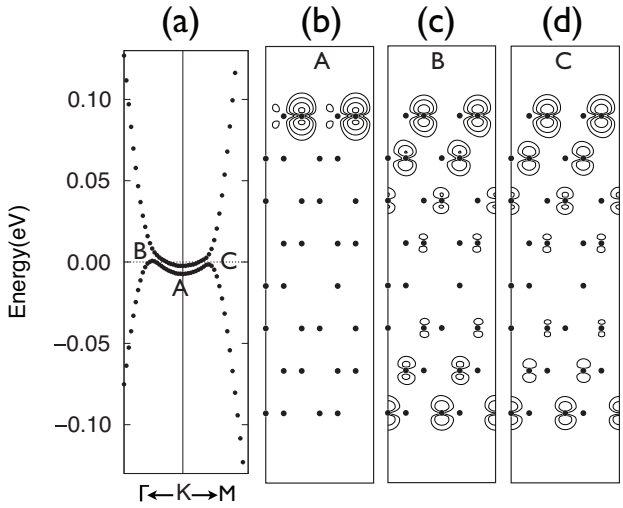


Figure 2: (a) Electronic energy band around the Fermi level in the vicinity of the $K$ point. (b)-(d) Contour plots of square wave function of highest occupied state at A, B, C points of eight atomic layer rhombohedral graphite slab with interlayer spacing 3.35 Å. The energy is measured from the Fermi level. The solid circles denote the positions of C atoms. Each contour represents twice (or half) the density of adjacent contour lines.

drastically changes its distribution: the polarized spins on two surfaces become coupled in parallel, leading to finite net spin moment for the thin film [Figs. 1(d)-1(f)]. Our calculations show that the transition between antiparallel and parallel spin coupling takes place at an interlayer spacing of about 3.0 Å. Note that the total-energy difference between the magnetic state and non-magnetic state of rhombohedral graphite film is about 1 meV/atom so that the magnetic state could be observed under very low temperature. Thus, by using appropriate experimental techniques, such a modulation in the magnetic properties could be detectable in thin films of graphite with the rhombohedral stacking arrangement. In sharp contrast to the relative spin arrangement between surfaces, on each surface the ferrimagnetic spin ordering is robust against the variation of the interlayer spacing and maintains its distribution even at considerably narrowed spacings. This ferrimagnetic spin distribution results in an invariable magnetic moment on the topmost or bottommost surface.

To clarify the mechanism that lies behind the magnetic property modulation of rhombohedral graphite thin films as a function of the decrease of the interlayer spacing, we investigated the electronic energy band and wave func-

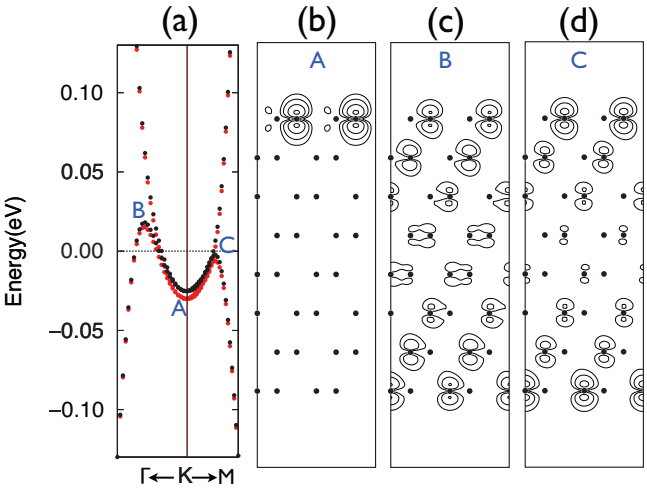


Figure 3: (a) Electronic energy band around the Fermi level in the vicinity of the $K$ point. (b)-(d) Contour plots of square wave function of highest occupied state at A, B, C points of eight atomic layer rhombohedral graphite slab with interlayer spacing 2.8 Å. The energy is measured from the Fermi level. Red (gray) and black dotted lines denote the electronic energy band for majority and minority spins, respectively. Each contour represents twice (or half) the density of adjacent contour lines.

tion distribution associated with the flat band states. Figures 2 and 3 show the electronic energy band and the squared wave functions in the vicinity of the $K$ point around the Fermi energy level of rhombohedral graphite slabs with interlayer spacings of d=3.35 Å and d=2.8 Å, respectively. It should be noted that the majority and minority spin states are degenerated in the case of the rhombohedral graphite slab with interlayer spacing of d=3.35 Å. At the $K$ point, the wave function completely localizes on the C atoms situated at the outermost atomic layer as shown in Figs. 2(b) and 3(b) irrespective of the interlayer spacing. The characteristic distribution corroborates the fact that this state is classified as an "edge state". Then, decreasing the wave number, or approaching the $\Gamma$ or $M$ points, the state loses its surface localized nature and the wave function gradually penetrates inside the slab as shown in Figs. 2(c), 2(d), 3(c), and 3(d). By comparing the wave function distribution of the edge states between the thin films with 3.35 Å and 2.8 Å interlayer spacings, it is clear that the penetration depth of the wave function for the narrower spacing is greater than that for the equilibrium spacing. This penetration depth of the wave function is considered to be the physical

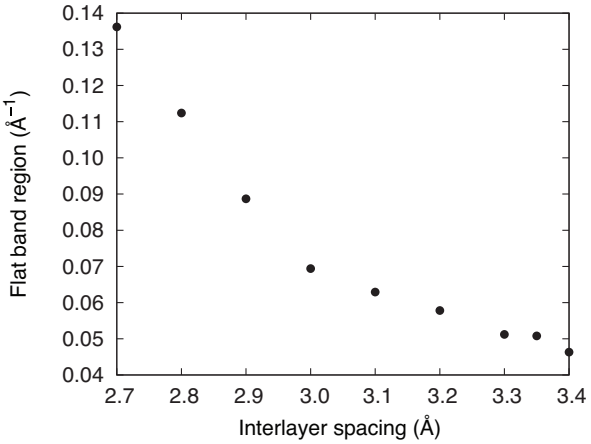


Figure 4: Interlayer spacing dependence of the flat-band region of a rhombohedral graphite slab with eight atomic layers.

origin for the different spin coupling. In the rhombohedral graphite slab with interlayer spacings of 3.35 Å, the wave function of the flat band state exhibit localized nature to the outer region of the film. On the other hand, it is clear that the penetration depth of the wave function for the narrower spacing is deeper than that for the equilibrium spacing. Indeed, non-negligible wave function overlap between orthogonalized degenerate flat band states, in the case of the thin film with narrower interlayer spacing. The overlap between the wave functions of the these flat band states on both surfaces causes Coulomb energy cost. By decreasing the interlayer spacing, the enhancement of the wave function overlap causes the increase of Coulomb energy. This results in the high spin state (non-zero magnetic moment state) to exclude the double occupancy of the $\pi$ states of each graphene layer (in a similar way as for Hund's rule for the $d$ orbitals in transition metal magnets), leading to the parallel spin coupling in the rhombohedral graphite thin films. [21] These results indicate that thin films of rhombohedral graphite should be applicable for magnetic devices where the magnetic properties are tunable by controlling the external pressure. Indeed, we estimated that the critical uniaxial pressure for a magnetic phase transition at interlayer spacing 3.0 Å is 7.5 GPa by using the relation $P = -dE/dV$, where the $V$ is the volume of the films. On the other hand, this fact also indicates the possibility that the magnetic properties depend not only on the interlayer spacing but also on the thickness of the slab.

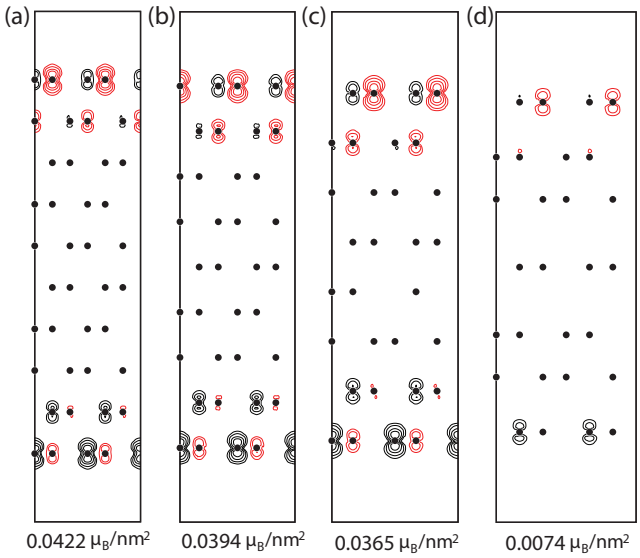


Figure 5: Contour plots of spin density and surface magnetic moment of rhombohedral graphite slabs with interlayer spacing 3.35 Å for (a) ten atomic layers, (b) nine atomic layers, (c) eight atomic layers, and (d) seven atomic layers. The solid circles denote the positions of C atoms. Positive and negative values of spin density are shown by red (gray) and black lines, respectively. Each contour represents twice (or half) the density of adjacent contour lines.

Another interesting issue is how the flat band region depends on the interlayer spacing. In previous work [10] based on the tight-binding approximation, it found that the flat band region increased with increasing interlayer electron transfer. We therefore estimated the flat-band region around the $K$ point as that defined by the distance between the A, B and C points in the energy band of the highest occupied state [Figs. 2(a), and 3(a)]. We found that the flat-band region monotonically increases with decreasing interlayer spacing, as shown in Fig. 4. This feature is ascribed to the fact that the interlayer spacing is directly associated with the interlayer electron transfer.

As pointed out above, the magnetic properties of thin films of rhombohedral graphite depend not only on the interlayer spacing but also on the film thickness. Thus, we next investigated the electronic and magnetic properties of rhombohedral graphite slabs whose thicknesses ranged from three to thirteen atomic layers. Our DFT calculations revealed that the thinner slabs with six or less layers are metallic with no magnetic ordering. The absence of the magnetic state is ascribed to the substantial interaction of

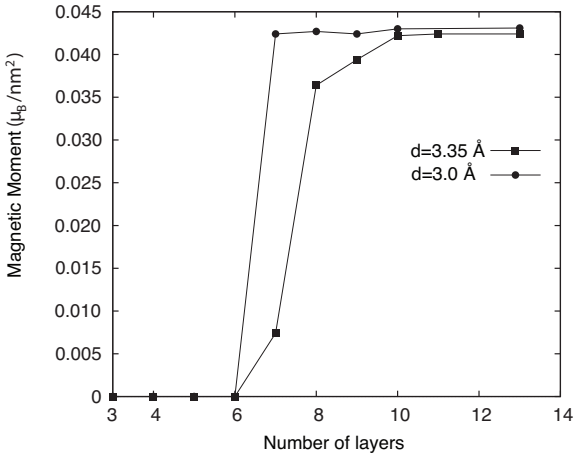


Figure 6: Surface magnetic moment of the rhombohedral graphite slab with interlayer spacing 3.35 Å (solid squares) and 3.0 Å (solid circles) as a function of the number of graphene layers.

wave functions between the topmost and the bottommost layers: although the wave function at the $K$ point completely localizes at the surface atomic site, the flat band state away from the $K$ point exhibits an extended nature so that there is substantial overlap between the two surfaces, leading to the metallic properties. When we increased the number of layers, we found that the magnetic state emerged as the ground state for the slab with seven or more layers. Figure 5 shows the spin density of graphite slabs with ten to seven atomic layers. All these graphite slabs possess magnetic ordering such that each surface exhibits ferrimagnetic spin ordering while the spins between the two surfaces are coupled in an antiparallel manner, as in the case for the spin distribution in graphene nanoribbons. In the seven layer slab, the calculated magnetic moments at the topmost and bottommost layers are very small, 0.0074 $\mu_{\rm B}$/nm$^2$ compared to those observed in the thicker slab. The magnetic moment of the topmost or the bottommost graphene layer strongly depends on the number of graphene layers.

It is worth to estimate whether the surface magnetic moment increase or not with further increase of the thickness of slabs. As shown in Fig. 5, among the slabs with seven to ten layers, the film comprising ten layers possesses the largest magnetic moment of 0.042 $\mu_{\rm B}$/nm$^2$. By investigating the magnetic moment for the slabs with eleven to thirteen layers, we find that the magnetic moment of about 0.04 $\mu_{\rm B}$/nm$^2$ is the saturated value for the rhombohedral

graphite thin film with equilibrium interlayer spacing (Fig. 6). The thickness dependence of magnetic moments of graphite slabs can be explained based on the penetration depth of the wave function associated with the flat dispersion band around the $K$ point, as in the case of graphene nanoribbons [3, 4].

Besides the graphene thin films with equilibrium interlayer spacing, we also find that the surface magnetic moment of the compressed slab exhibits similar the thickness dependence. Indeed, the compressed graphite thin films with the interlayer spacing of 3.0 Å also do not exhibit the magnetic ordering with six or less atomic layers. While the finite magnetic moment of about 0.04 $\mu_{\rm B}/{\rm nm}^2$ is found for the slabs with seven or much layers, and then these values are almost unchanged with increasing the number of atomic layers as in the case of the thin films with equilibrium interlayer spacing (Fig. 6).

The substrates or mediums are essential to apply the pressure on the graphite thin films. Therefore, we investigated the effect of substrate on the magnetic properties of graphite thin film under the uniaxial compression. We considered the model in which the graphite thin film is sandwiched by two hexagonal boron-nitride ($h$-BN) sheets simulating the insulating substrate or pressure mediums. We chose 2 Å spacing between $h$-BN and the topmost/bottommost graphene layer to simulate the strong coupling limit between substrate and graphite. Figure 7 shows the contour plot of polarized electron spin density of ten atomic layer rhombohedral graphite thin film with 3.0 Å interlayer spacing sandwiched by two $h$-BN layers. We find that the electron spin density dismisses at the topmost and the bottommost graphene layers situated at interface with substrate due to the strong interaction. However, we still observe the polarized electron spins on the subsurface layers of graphite thin film. The polarized spins on these surfaces are coupled in parallel. The calculated surface magnetic moment is found to be 0.042 $\mu_{\rm B}/{\rm nm}^2$. This result corroborates our above results for the free-standing graphite thin films. Therefore, the magnetic properties of graphite thin film are certainly tunable by the external pressure.

## 4. Summary

Based on first-principles total energy calculations, we studied the magnetic properties of thin films of graphite with the rhombohedral stacking arrangement in terms of the interlayer spacing and film thickness. We found that the ferrimagnetic spin ordering on the outermost atomic layer is robust against variations in interlayer spacing and number of graphene layers. On

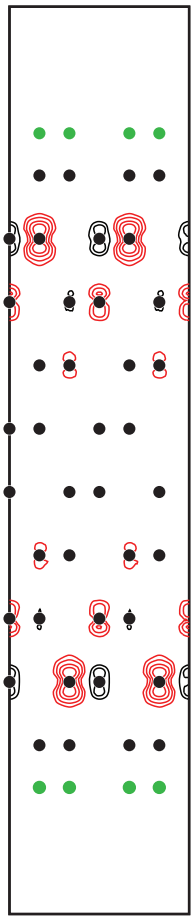

Figure 7: Contour plot of spin density of ten atomic layer rhombohedral graphite thin film sandwiched by two $h$-BN layers with graphene interlayer spacing of 3.0 Å. The black solid circles denote the position of C atoms. The green solid circles denote the position of B/N atoms. Positive and negative values of spin density are shown by red (gray) and black lines, respectively. Each contour represents twice (or half) the density of adjacent contour lines.

the other hand, antiparallel spin coupling between the top and bottom surfaces is drastically affected by decreasing the interlayer spacing. Below an interlayer spacing of 3 Å, the polarized electron spins between the two surfaces are coupled in parallel, leading to a finite magnetic moment on these rhombohedral graphite thin films. Detailed analysis of the wave function of the flat band states unravelled the mechanism of this modulation of magnetic ordering: the increase in interlayer interaction leads to the enhancement of overlap of wave functions associated with the flat band states of the two surfaces.

We also demonstrated that the surface magnetism on rhombohedral graphite film depends on the slab thickness. Regardless the interlayer spacing, thin films of rhombohedral graphite with six or fewer graphene layers are metallic, without any magnetic ordering. Increasing the number of layers to seven or more leads to films which possess magnetic ordering such that each surface exhibits ferrimagnetic spin ordering while the spins between the two surfaces are coupled in an antiparallel manner, as has also been found for the spin distribution in graphene nanoribbons. Furthermore, the surface magnetic moment gradually increases with increasing number of graphene layers, and saturates at ten atomic layer with the surface moment of 0.04 $\mu_{\mathrm{B}}/\mathrm{nm}^2$. In addition, we also clarify the substrate effect on the magnetic properties of graphite thin film. Although, the substrate suppresses the magnetism on the topmost and the bottommost layer of graphite, we find qualitatively the similar magnetic ordering on the second sublayers of graphite. The result opens the possibility for tuning the magnetic properties of thin films of graphite by controlling the external pressure.

## Acknowledgments

This work was partly supported by CREST, Japan Science and Technology Agency, and a Grant-in-Aid for scientific research from the Ministry of Education, Culture, Sports, Science and Technology of Japan.

## Supplementary data

The exact atomic coordinates of rhombohedral graphite thin films used in this paper can be found online at doi:X.X/X.X.X.X

## References


[1] N. Hamada, S. I. Sawada, A. Oshiyama, Phys. Rev. Lett. 68 (1992) 1579.

[2] R. Saito, M. Fujita, G. Dresselhaus, M. S. Dresselhaus, Appl. Phys. Lett. 60 (1992) 2204.

[3] M. Fujita, K. Wakabayashi, K. Nakada, K. Kusukabe, J. Phys. Soc. Jpn. 65 (1996) 1920.

[4] K. Nakada, M. Fujita, G. Dresselhaus, M. S. Dresselhaus, Phys. Rev. B 54 (1996) 17954.

[5] K. Wakabayashi, M. Sigrist, M. Fujita, J. Phys. Soc. Jpn. 67 (1998) 2089.

[6] S. Okada, M. Igami, K. Nakada, A. Oshiyama, Phys. Rev. B 62 (2000) 9896.

[7] S. Okada, A. Oshiyama, Phys. Rev. Lett. 87 (2001) 146803.

[8] Y. Miyamoto, K. Nakada, M. Fujita, Phys. Rev. B 59 (1999) 9858.

[9] M. Koshino, E. McCann, Phys. Rev. B 80 (2009) 165409.

[10] M. Otani, M. Koshino, Y. Takagi, S. Okada, Phys. Rev. B 81 (2010) 161403 (R).

[11] M. Otani, Y. Takagi, M. Koshino, S. Okada, Appl. Phys. Lett. 96 (2010) 242504.

[12] Y. Takagi, J. Phys. Soc. Jpn. 78 (2009) 064701.

[13] Y. Takagi, S. Okada, Surf. Sci. 602 (2008) 2876.

[14] P. Hohenberg, W. Kohn, Phys. Rev. 136 (1964) B864.

[15] W. Kohn, L. J. Sham, Phys. Rev. 140 (1965) A1133.

[16] J. P. Perdew, A. Zunger, Phys. Rev. B 23 (1981) 5048.

[17] D. M. Ceperley, B. J. Alder, Phys. Rev. Lett. 45 (1980) 566.

[18] D. Vanderbilt, Phys. Rev. B 41 (1990) 7892.

[19] M. Otani, O. Sugino, Phys. Rev. B 73 (2006) 115407.

[20] I. Hamada, M. Otani, O. Sugino, Y. Morikawa, Phys. Rev. B 80 (2009) 165411.

[21] S. Okada, A. Oshiyama, J. Phys. Soc. Jpn. 72 (2003) 1510.